

Specific Targeting of Hepatitis C Virus NS3 RNA Helicase. Discovery of the Potent and Selective Competitive Nucleotide-Mimicking Inhibitor QU663[†]

Giovanni Maga,^{‡,§} Sandra Gemma,^{§,||} Caterina Fattorusso,^{§,⊥} Giada A. Locatelli,^{‡,§} Stefania Butini,^{§,||} Marco Persico,^{§,⊥} Gagan Kukreja,^{§,||} Maria Pia Romano,^{§,||} Luisa Chiasserini,^{§,||} Luisa Savini,^{§,||} Ettore Novellino,^{§,⊥} Vito Nacci,^{§,||} Silvio Spadari,^{‡,§} and Giuseppe Campiani^{*,§,||}

Istituto di Genetica Molecolare, CNR-Pavia, via Abbiategrasso 207, 27100 Pavia, Italy, European Research Centre for Drug Discovery and Development, Università' di Siena, Banchi di Sotto 55, 53100 Siena, Italy, Dipartimento Farmaco Chimico Tecnologico, Università' di Siena, via Aldo Moro, 53100 Siena, Italy, and Dipartimento di Chimica delle Sostanze Naturali and Dipartimento di Chimica Farmaceutica e Tossicologica, Università' di Napoli Federico II, via D. Montesano 49, 80131 Napoli, Italy

Received December 7, 2004; Revised Manuscript Received April 4, 2005

ABSTRACT: Hepatitis C virus (HCV) infection is an emerging global epidemic, and no effective cure is yet available. Interferon- α (INF α) and pegylated INFs, in combination or otherwise with ribavirin, have proven to be effective in no more than 50% of chronically infected patients. New and better therapeutic strategies are therefore needed. HCV nonstructural protein 3 (NS3) RNA helicase (h) is a promising target for developing new therapeutics. QU663 was discovered as a potent new selective inhibitor of the helicase reaction of HCV NS3 ($K_i = 0.75 \mu\text{M}$), competing with the nucleic acid substrate without affecting ATPase function, even at high concentrations. QU663 is one of a new generation of small-molecule nucleotide-mimicking inhibitors which are potential anti-HCV agents. A thorough molecular modeling study was carried out to explain the molecular basis of NS3h inhibition by QU663. The resulting three-dimensional interaction model is discussed.

Hepatitis C virus infection is a serious health problem, affecting ~170 million people worldwide (1). Patients may develop chronic hepatitis, liver cirrhosis, and end-stage liver disease (1, 2). The only available therapy for HCV¹ is based on INF α , either alone or in combination with the nucleotide analogue ribavirin. This therapy has a success rate of $\leq 50\%$, and its use is limited by severe side effects. It is therefore necessary to find alternative drugs which selectively interact with an enzyme of the viral replication complex, blocking viral growth with little or no toxicity for uninfected host cells.

The agent of hepatitis C is the HCV virus, the genome of which contains a single open reading frame (ORF) encoding a single polyprotein that is processed by virus-encoded and host cellular proteases into structural and nonstructural (NS) proteins (1, 2). One NS protein is the protease/helicase NS3, a multifunctional enzyme with serine-protease and NTPase/

helicase activities implicated in processing of the viral polyprotein and duplication of the HCV genome (3). NTPase activity hydrolyzes ribo- and deoxy-NTPs, as well as nucleoside triphosphate analogues. Hydrolysis of nucleoside triphosphates is believed to supply energy for the unwinding reaction carried out by helicase (3). Like NTPase activity, that of helicase of NS3 has broad substrate specificity, unwinding DNA–DNA and RNA–RNA homoduplexes, as well as RNA–DNA heteroduplexes. This peculiar lack of substrate specificity of NS3 NTPase and helicase activities makes identification of a specific inhibitor a challenging task (3).

Two classes of NS3 NTPase/helicase inhibitors are currently being developed, and are divided into competitive and noncompetitive, according to their mechanism of action. Competitive inhibitors are nucleotide analogues such as ribavirin 5'-triphosphate (RTP) and adenosine 5'- γ -thiotriphosphate (ATP- γ -S), which prevent binding of ATP to the enzyme, and some piperidine derivatives and heterocyclic substituted carboxanilides. Several polynucleotides and various RNA aptamers are also reported to inhibit helicase activity by a competitive mechanism, but their therapeutic potential is limited.

Some molecular dimers that seem to act at the nucleic acid (NA) binding site without affecting NTPase activity were recently reported (4). Compounds that do not interfere directly with substrate binding but inhibit the NTPase/helicase activity by other mechanisms belong to the class of noncompetitive inhibitors. For example, some DNA–RNA intercalators, such as anthracycline and mitoxantrone, can prevent translocation of NS3h along the polynucleotide chain by enhancing the rigidity or inducing deformation of the

[†] This work was partially supported by EU Grant LSHB-CT-2003-503480-TRIoh (to G.M.).

* To whom correspondence should be addressed. Telephone: 0039-0577-234172. Fax: 0039-0577-234333. E-mail: campiani@unisi.it.

[‡] CNR-Pavia.

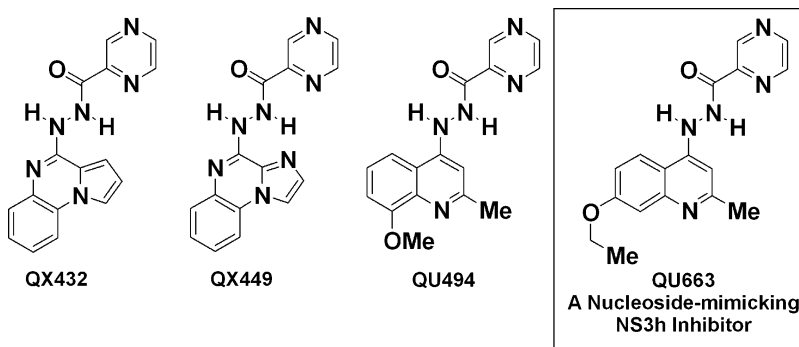
[§] European Research Centre for Drug Discovery and Development, Università' di Siena.

^{||} Dipartimento Farmaco Chimico Tecnologico, Università' di Siena.

[⊥] Università' di Napoli Federico II.

¹ Abbreviations: HCV, hepatitis C virus; NS3, nonstructural protein 3; TP, template–primer; NA, nucleic acid; HIV, human immunodeficiency virus; N⁹-CEG, N⁹-chloroethylguanine; QU663, N'-(pyrazinecarbonyl)-N''-(7-ethoxy-2-methylquinolin-4-yl)hydrazine; QX449, N'-(pyrazinecarbonyl)-N''-(imidazo[1,2-a]quinoxalin-4-yl)hydrazine; QX432, N'-(pyrazinecarbonyl)-N''-(pyrrolo[1,2-a]quinoxalin-4-yl)hydrazine; QU494, N'-(pyrazinecarbonyl)-N''-(8-methoxy-2-methylquinolin-4-yl)hydrazine.

Chart 1



structure of DNA or RNA substrates (1, 2). Finally, N⁹-CEG inhibits viral replication, probably by a feedback mechanism, inducing overproduction of ssRNA, the substrate of viral polymerase.

To find novel candidate molecules that could inhibit NS3 helicase (NS3h) and NTPase activities, we considered the similarity of HIV and HCV (5), and screened selected known compounds that target the non-nucleoside HIV-1 reverse transcriptase (RT) binding site (6, 7). Among the molecules that were tested, we identified QX432 (Chart 1), a quinoxaline-based inhibitor of HIV-1 reverse transcriptase and HCV NS3h. Lead optimization, based on molecular modeling and biological studies, led to the identification of quinoline QU663, which potently and selectively inhibits the helicase reaction in a competitive manner with respect to the NA substrate, without affecting ATPase function, making it a promising candidate for a novel class of anti-HCV drugs. The development of QU663, its putative binding site, key interactions within NS3h, and pharmacological properties are discussed.

MATERIALS AND METHODS

Quinoxalines (Chart 1) QX432 and QX449 were synthesized by standard methods, while quinolines QU494 and QU663 were synthesized starting from *m(o)*-phenetidine (Supporting Information).

Preparation of Nucleic Acid Substrates. For the preparation of the 5'-end-labeled sp d18:d66-mer DNA substrate, the d18-mer primer was labeled with bacteriophage T4 polynucleotide kinase (Ambion) and [γ -³²P]ATP, according to the manufacturer's protocol. After removal of unincorporated ATP on a Sephadex G-25 column, the appropriate 5'-end-labeled primer was mixed at a 1:1 molar ratio with the d66-mer template in 20 mM Tris-HCl (pH 8.0), containing 20 mM KCl and 1 mM EDTA, heated at 65 °C for 5 min, and then slowly cooled to room temperature. Concentrations of d66-mer and d18-mer were calculated from their molar extinction coefficients (758 760 and 193 820 M⁻¹ cm⁻¹, respectively). For details on the oligonucleotide sequences, see the Supporting Information.

Protein Purification. *Escherichia coli* DH5 α was cotransformed with plasmid pAW3 encoding His-tagged NS3. A 50 mL culture was grown overnight in LB broth (pH 7.5) at 37 °C. A 45 mL aliquot of the overnight culture was used to inoculate a 500 mL culture in LB broth (pH 7.5) at 37 °C. The culture was grown to an absorbance of 0.5 and then induced with IPTG (0.5 mM). Induction proceeded for 3 h at 25 °C, and then the cells were harvested by centrifugation

at 4000 rpm for 15 min in a Beckman JA20 rotor. Cell lysis was performed in buffer A [50 mM NaH₂PO₄ (pH 8.0), 300 mM NaCl, and 100 mM imidazole]. The lysate was sonicated and the suspension centrifuged at 9000 rpm for 10 min in a Beckman JA20 rotor. NS3 was purified from the supernatant by chromatography through a FPLC–NiNTA column, first washed for 40 min with 10 mL of buffer B [50 mM NaH₂PO₄ (pH 8.0), 300 mM NaCl, and 20 mM imidazole]. NS3 bound to the column was eluted with buffer B containing 250 mM imidazole. Fractions containing NS3 were identified by a SDS–PAGE gel assay. The concentration of homogeneous HCV NS3 was determined spectrophotometrically using a molar extinction coefficient of 64 200 M⁻¹ cm⁻¹.

ATPase Assays. NTPase activity was determined as previously described (8), directly monitoring [γ -³²P]ATP hydrolysis by thin-layer chromatography. A final volume of 5 μ L contained 100 nM NS3, 50 μ M polyuridylic acid, and 0.33 μ M [γ -³²P]ATP. Samples were incubated for 30 min at 25 °C and dotted onto sheets of PEI-cellulose. The products were separated by ascending chromatography with 0.5 M KH₂PO₄ (pH 3.4). Intensities of the radioactive bands corresponding to ATP and P_i were quantified by densitometric scanning with a PhosphorImager.

Helicase Assays. The NS3h assay was performed as previously described (8, 9) in a 15 μ L reaction volume containing 200 nM NS3, 5 mM Tris-HCl (pH 7.5), 5 mM MgCl₂, 25 nM ³²P-labeled partial duplex DNA substrate, and 5 mM ATP. The reaction mixture was incubated for 20 min at 25 °C, and then the reaction was stopped with 10 μ L of termination buffer [10% (w/v) glycerol, 0.0015% (v/v) bromophenol blue, 0.0015% (w/v) xylene cyanol FF, and 10 mM EDTA]. Aliquots were analyzed on a native 8% (w/v) polyacrylamide gel. Intensities of radioactive bands corresponding to ds18:66-mer and ss18-mer were quantified by densitometric scanning with a PhosphorImager. For spectrophotometric measurements, absorbance at 260 nM was measured with an Ultrospec 2001*pro* spectrophotometer (Amersham Biosciences) in a 300 μ L quartz cuvette. A final volume of 300 μ L contained 20–50 nM NS3, 50 mM Tris-HCl (pH 7.5), 5 mM MgCl₂, and NA as indicated in the figure legends. Samples containing the enzyme without NA substrate were measured, and the absorbance was subtracted to obtain the increase in AU (FAU). Helicase reactions were started by addition of enzyme. Samples were equilibrated at room temperature (25 °C) before measurement. Each measurement was repeated at least three times and the mean used for interpolation. For absorbance quenching experiments, a final volume of 300 μ L contained 50 mM Tris-HCl (pH 7.5),

5 mM MgCl₂, QU663, and NA as indicated in the figure legends. DNAase I partially digested calf thymus DNA had a mean fragment length of 250 bp, as determined by agarose gel electrophoresis.

Electrophoretic Mobility Shift Assays. A 15 μ L reaction volume contained 50 mM Tris-HCl (pH 7.5), 5 mM MgCl₂, 5 mM ATP, QU663, and DNA substrate (pTrc plasmid, 4.4 kb, InvitroGen) as indicated in the figure legends. The reaction mixture was incubated for 20 min at 25 °C and then the reaction stopped with 10 μ L of gel loading buffer [10% (w/v) glycerol, 0.0015% (v/v) bromophenol blue, 0.0015% (w/v) xylene cyanol FF, and 10 mM EDTA]. Samples were run on a 0.75% agarose gel in the absence of EtBr.

Inhibition Assays and Determination of Kinetic Constants. Inhibition assays for ATPase and helicase activity were performed under the conditions described for ATPase and helicase activity assay, in the presence of increasing amounts of the inhibitor (10, 20, 50, 100, 200, and 500 μ M) and different concentrations of DNA substrate (33, 66, and 333 nM). Time course experiments were performed as described in the figure legends. Data were analyzed according to the exponential equation

$$\text{FAU} = A(1 - e^{-k't})$$

where A is the burst amplitude, k' the apparent first-order rate constant for association of the enzyme with its substrate (burst rate), and t time.

The apparent catalytic rate k'_{max} of the reaction and the enzyme affinity for NA substrate (K_{NA}) were calculated according to the relationship

$$k' = k'_{\text{max}}[\text{NA}]/([\text{NA}] + K_{\text{NA}})$$

Dose–response curves were analyzed according to Hill's model, to take into account the cooperative binding of NS3 to the DNA substrate. The ID₅₀ (concentration of inhibitor causing 50% inhibition) was calculated by fitting the experimental data to the equation (9)

$$k' = k'_{\text{max}}/(1 + ([\text{I}]/\text{ID}_{50})^n)$$

where k' is the reaction rate in the presence of inhibitor concentration $[\text{I}]$, k'_{max} the reaction rate in the absence of the inhibitor, and n the cooperativity index.

Since the enzyme concentration in the reaction was high and not negligible with respect to DNA substrate concentration, K_i could not be derived from ID₅₀ through the Cheng–Prusoff relationship for competitive inhibitors. ID₅₀ values were therefore converted to K_i values according to the equation (10)

$$K_i = [\text{ID}_{50}/([E] - K_d^{1/n} - 0.5n[E]) - 1]K_d^{1/n}$$

where $[E]$ is total enzyme concentration, K_d the dissociation constant for DNA binding, and n the cooperativity index.

Molecular Modeling. All molecular modeling studies are reported as Supporting Information.

HIV-1 RT Inhibition Assays, Secondary Anti-HIV Tests (Cell Culture Assays), and Toxicity Tests. All the experiments are reported as Supporting Information.

RESULTS AND DISCUSSION

QU663 Is a Specific Inhibitor of Strand Displacement Activity of HCV NS3 Protein. We tested its ability to inhibit

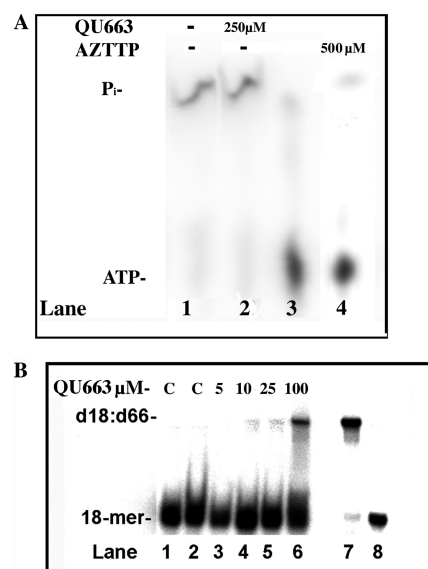


FIGURE 1: Inhibition of NS3 ATPase and helicase activities by QU663. For assay conditions, see Materials and Methods. (A) Chromatogram of an ATPase reaction in the absence (lane 3) or in the presence of radioactive ATP at 0.5 mM (lanes 1 and 2) and increasing concentrations of QU663. The positions of the radioactive spots corresponding to the substrate (ATP) and the product (P_i) are indicated on the left side of the panel. Lane 4 contained a positive control in the presence of 500 μ M AZTTP. (B) Denaturing polyacrylamide gel electrophoretic analysis of the products of a helicase assay in the presence of increasing concentrations of the QU663 inhibitor (lanes 1–6). Lane 7 contained a reaction mix incubated without enzyme. Lane 8 contained a boiled mixture.

the NTPase and helicase activities of NS3. In the NTPase assay, γ -phosphate-labeled ATP was incubated with purified NS3 and the reaction products were resolved by TLC. From the chromatogram of Figure 1A, it was clear that QU663 was unable to inhibit NS3 NTPase activity, even at high concentrations. Figure 1B shows the results of a typical helicase assay. A radiolabeled d18:d66-mer substrate (see Materials and Methods) was incubated with NS3 without or with increasing concentrations of QU663. The double-stranded template was then separated from the displaced ssd18-mer oligonucleotide by native PAGE. As indicated by the increase in the magnitude of the signal of the double-stranded substrate, QU663 significantly inhibited helicase activity of NS3 at a concentration of 100 μ M.

QU663 Is a Competitive Inhibitor of NS3h with Respect to NA Substrate. As shown in Figure 1, QU663 inhibited strand displacement activity of NS3 without affecting its ability to hydrolyze ATP. The hypothesis that QU663 inhibited NA substrate utilization was tested by spectrophotometric assays of variations in absorbance due to the double-to single-strand transition of NA in the presence of NS3. The assays were performed in the presence of different concentrations of d18:d66-mer substrate and different concentrations of QU663. As shown in Figure 2A, in the absence of QU663 and in the presence of 66 nM NA, the absorbance increased in a time-dependent manner as a consequence of unwinding of the substrate by NS3. Similar experiments were performed with three different concentrations of QU663. As shown in panels A and B of Figure 2, QU663 inhibited unwinding of NA in a dose-dependent manner. When a fixed concentration of QU663 was tested in the presence of increasing d18:d66-mer concentrations, the level of inhibition

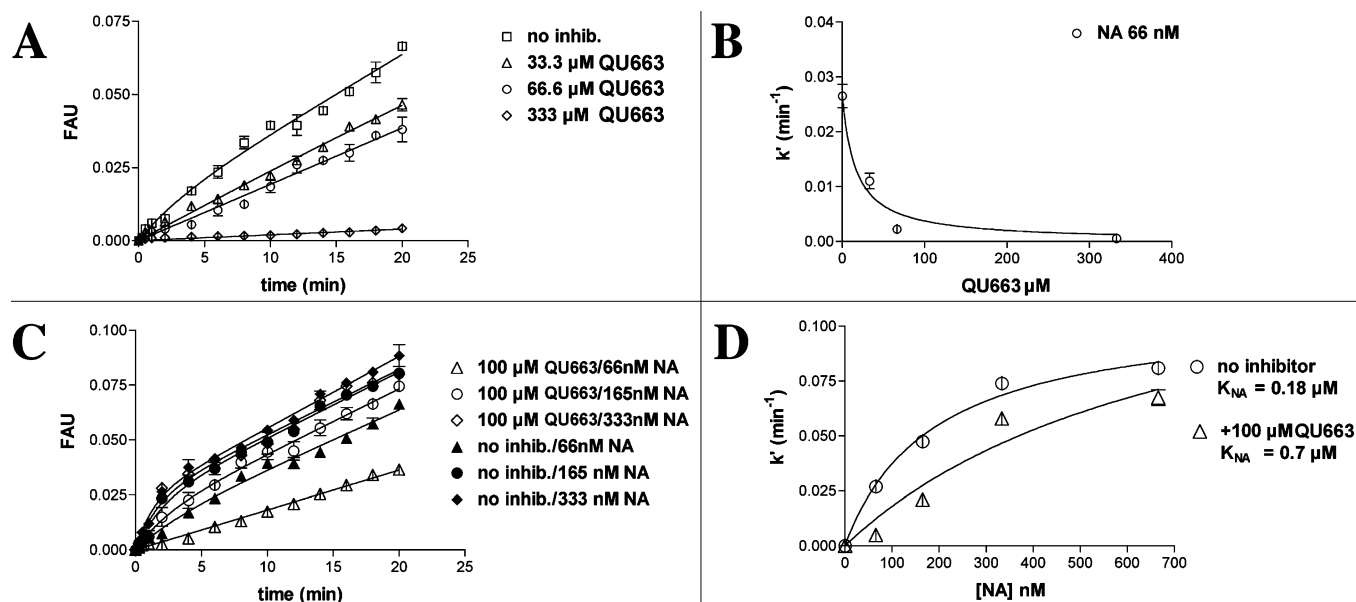


FIGURE 2: Inhibition of the NS3h activity by QU663 is competitive with the DNA substrate. (A) Analysis of the absorbance profile for the NS3-catalyzed helicase reaction, in the presence of 66 nM NA and in the absence (\square) or presence of increasing concentrations [33.3 (Δ), 66.6 (\circ), and 333 μM (\diamond)] of QU663. (B) Dose-response curve for the inhibition of the NS3h reaction by QU663. The apparent velocity values (k') were derived as described in Materials and Methods. (C) Dependence of QU663 inhibition of the helicase reaction on NA concentration. Reactions were performed and followed spectrophotometrically in the presence of three concentrations of NA [66 (triangles), 165 (circles), 333 nM (diamonds)] in the absence (black symbols) or presence (white symbols) of 100 μM QU663. (D) Variation of the apparent affinity of NS3 for the NA (K_{NA}) as a function of QU663 concentration. The variation of the reaction velocity k' was determined in relation to QU663 concentration, in the absence (\circ) or presence (Δ) of 100 μM QU663. The calculated K_{NA} values are on the right side of the panel.

Table 1: Inhibition of HCV NS3h and HIV-1 RT wt by QX432, QX449, QU494, and QU663

compd	K_i for inhibition of HCV NS3h (μM)	K_i for inhibition of HIV-1 RT wild type (μM)
QX432	22.3	0.19
QX449	4.5	5.5
QU494	15.6	> 50
QU663	0.75	NA ^a

^a Not active at 10^{-4} M.

decreased with an increase in NA concentration (Figure 2C). When the effect of the same QU663 concentration on the apparent affinity of NS3 for d18:d66-mer substrate was checked, QU663 seemed to decrease the affinity of the enzyme for NA substrate (Figure 2D). Together, these results indicated that QU663 was a competitive inhibitor of NS3h activity, with respect to the NA substrate. Similar experiments performed at different substrate or inhibitor concentration ratios gave an estimated inhibition constant (K_i) of 0.75 μM (see Materials and Methods) for inhibition of NS3h activity by QU663. The same experimental approach was used to determine the mechanism of action of QX432, QX449, and QU494 (Table 1). None inhibited the ATPase activity of NS3, but they showed competitive inhibition of NS3h with respect to NA substrate (data not shown).

To determine whether QU663 itself binds to DNA, two standard approaches were used: absorbance quenching measurements and electrophoretic mobility shift assays. QU663 alone showed two distinct absorbance peaks: $\lambda_1 = 314$ nm and $\lambda_2 = 390$ nm (Figure 3A). When a fixed amount of QU663 was mixed with a different large molar excess of DNA, no quenching of λ_1 and λ_2 absorbance peaks of QU663 occurred in the presence of DNA (Figure 3B). When a large excess of QU663 was incubated with a DNA plasmid and

the mixture resolved in the absence of EtBr on a 0.7% agarose gel and stained with EtBr after the run and the position of the DNA revealed by UV shadowing, no differences in the mobility of supercoiled (sc) or nicked circular (nc) plasmid DNA were detected (Figure 3C). Together, these results indicated that QU663 did not bind DNA.

QU663, a Nucleotide-Mimicking NS3h Inhibitor. Starting from the class of ethylthioureidic anti-HIV agents (7), characterized, in some cases, by weak dual activity against HIV-1 RT and HCV NS3h (e.g., QX432, Table 1), we developed a new class of potent, selective, nucleotide-mimicking NS3h inhibitors, of which we discuss a representative set of quinoline (QU) and quinoxaline (QX) analogues (Table 1), typified by QU663. Through concerted effort involving synthesis, computational studies, and biological evaluation, the parent structure of HIV/HCV enzyme inhibitor QX432 (HIV-1 RT $K_i = 0.19 \mu\text{M}$; NS3h $K_i = 22.3 \mu\text{M}$) was progressively modified to obtain selective NS3h inhibitors. This study allowed us to identify the 2,4,7-trisubstituted quinoline skeleton as the optimal heterocyclic system for selective NS3h inhibitory activity. Interestingly, QX432 showed a peculiar electron distribution, calculated by the AM1 quantum mechanical method (see Materials and Methods), which determines the presence of a partially negative charged area around the hydrazide moiety (panel D of Figure 1SI of the Supporting Information), in perfect agreement with calculated apparent acidity constant ($\text{p}K_a$) values (Table 1 of the Supporting Information). To investigate the importance of this structural feature in terms of inhibitory activity and selectivity, we designed compound QX449, with an additional nitrogen atom in position 3 and a calculated higher percentage of the ionized form (Table 2

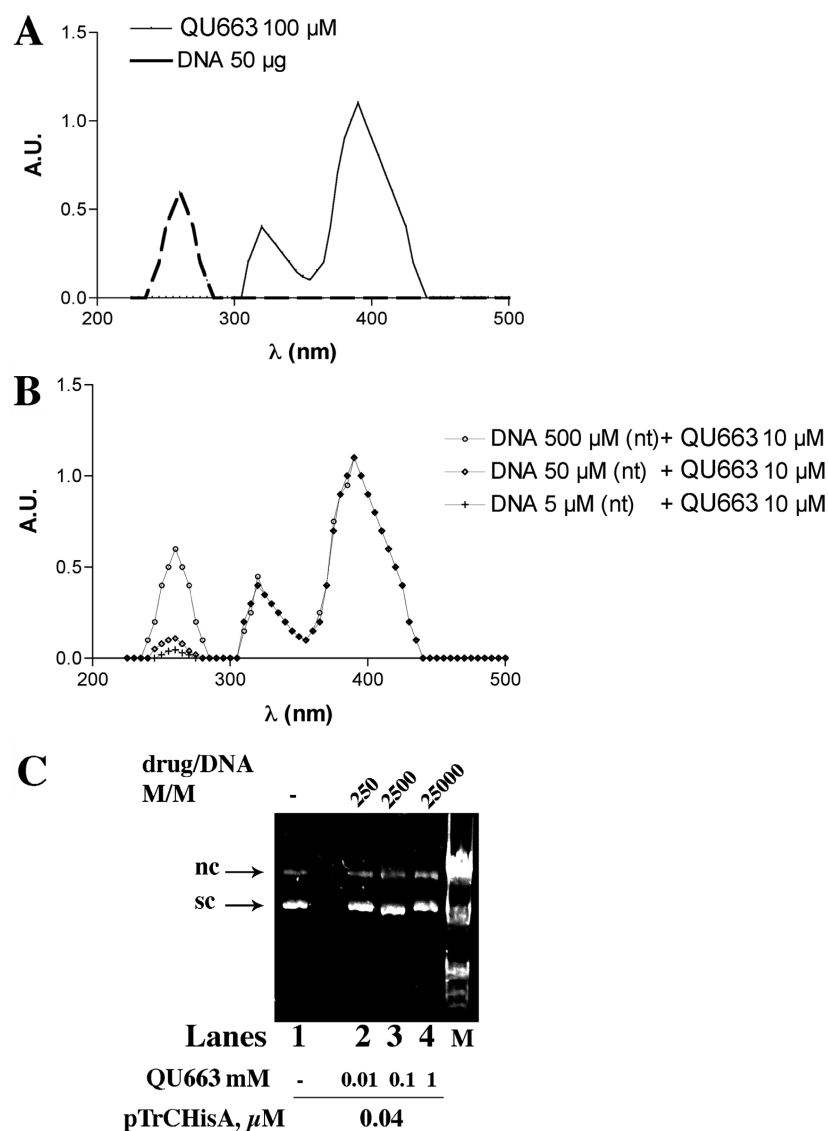


FIGURE 3: QU663 does not interact with DNA. (A) Absorbance peak determination for QU663 and ctDNA. Measurements were performed in the presence of 100 μ M QU663 (—) or 50 μ g of ctDNA (---). (B) Absorbance quenching determination for DNA/QU663 mixtures. Samples were prepared by mixing 10 μ M QU663 with ctDNA at the final concentrations (as nucleotides) of 5 (+), 50 (◇), and 500 μ M (○). (C) The 4.4 kb plasmid pTrCHisA at 0.04 μ M (InvitroGen) was mixed with 0.01 (lane 2), 0.1 (lane 3), and 1 mM QU663 (lane 4). Samples were prepared and analyzed by electrophoresis: lane 1, pTrCHisA alone; lane M, λ DNA Eco/Hind molecular size markers.

of the Supporting Information). QX449 turned out to be 5 times more active than QX432 against NS3h (NS3h K_i = 4.5 μ M, Table 1), indicating the importance of the above-mentioned negatively charged area, which could reproduce the negative charge of each monomer present in the NA substrate. To test the importance of reproducing on a synthetic small molecule compound the electronic distribution of purine and pyrimidine nucleotides, which have a positively charged area \sim 5.8 and \sim 7.3 Å from the phosphate moiety, respectively, we developed compounds QU494 and QU663, both characterized by a substituted quinoline system, but with different steric, electronic, and acidity properties related to the different position of the alkyloxy group (panel A vs panel B of Figure 1SI of the Supporting Information). In particular, QU494, which is endowed with apparent pK_a values similar to those of QX432 (Tables 1 and 3 of the Supporting Information), showed similar inhibitory activity against NS3h to QX432 (for QX432, K_i = 22.3 μ M, and for QU494, K_i = 15.6 μ M). Both QX449 and QU494 had lower K_i values for inhibition of HIV-1 RT, equal to 5.5 and >50

μ M, respectively (for QX432 HIV-1 RT, K_i = 0.19 μ M) (Table 1). Introduction of an ethoxy function at C-7 in the quinoline nucleus led to QU663, a selective NS3h inhibitor with sub-micromolar activity (K_i = 0.75 μ M), one of the most potent selective competitive inhibitors of NS3h. Electronic distribution and pK_a calculations for QU663 revealed some peculiarities: (i) a significant degree of protonation of the quinoline nitrogen at physiological pH (panel A of Figure 1SI and Table 4 of the Supporting Information) and (ii) a strong propensity of the hydrazide moiety to be negatively charged due to loss of a hydrogen (panel A of Figure 1SI and Table 4 of the Supporting Information), with (iii) a calculated distance between these highly polar centers of 5.92–6.23 Å, depending on the selected conformer. According to our hypothesis, these electronic and conformational features resemble those calculated for RNA–DNA nucleotides, which form the natural NS3h substrates (Figure 4). QU663 is therefore likely to be the first example of a nucleotide-mimicking competitive inhibitor of NS3h function. QU663 tested on HIV-1 reverse transcriptase (RT) and

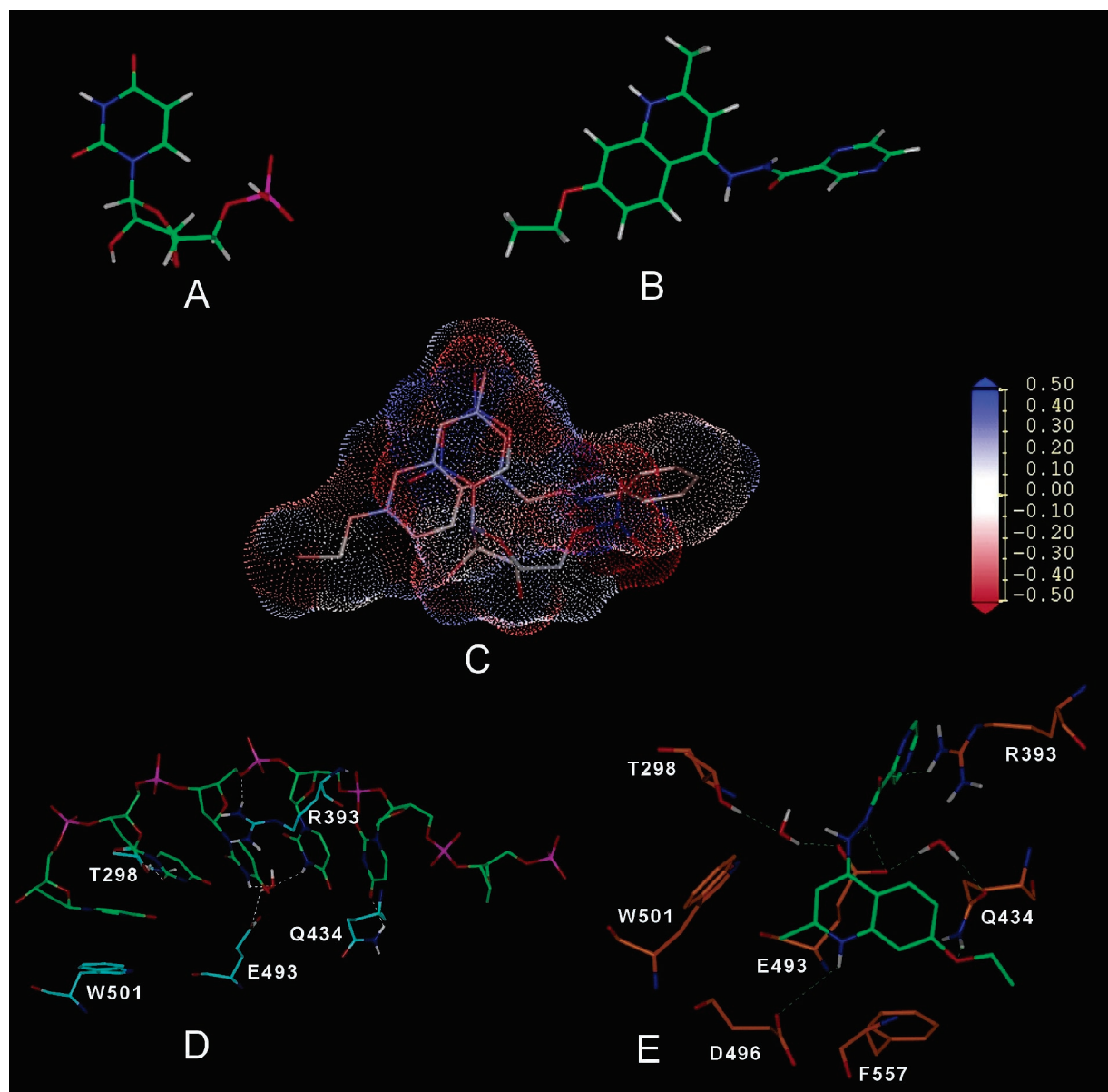


FIGURE 4: (A and B) Resulting MOPAC (AM1) conformers of 5'-UMP (A) and QU663 (B), colored by atom type (green for C, white for H, red for O, and blue for N). (C) Superimposition of 5'-UMP and QU663 by fitting their electronic distribution, colored according to AM1 partial charges. Connolly surfaces are displayed. (D and E) Ligand-enzyme main interactions in the NS3h-dU₈ X-ray complex (D) and QU663 docked into the putative NS3h binding site (E). The color code of dU₈ and QU663 follows: cyan (D) and orange (E) for NS3h carbons. All hydrogens, except those involved in hydrogen bonds (green dashed lines), have been omitted for clarity.

on the reaction intermediate formed by RT complexed with the DNA and nucleotide substrates did not show affinity and was devoid of any anti-HIV activity (Table 1). QU663 did not show cytotoxicity toward 3T3 cells, NSO cells, Daudi cells, and normal human lymphocytes (Supporting Information).

Docking Studies. A thorough inspection of available X-ray structures of NS3h (PDB entries 1A1V, 8OHM, 1HEI, and 1CU1) was performed for insights into a possible binding site for the most potent inhibitor, QU663. Since QU663 is a competitive DNA substrate inhibitor that selectively influences helicase activity, without affecting ATPase activity, all available mutagenesis research data were perused (refs 4–9 of the Supporting Information). As a result, we excluded all NS3h regions involving residues known to affect ATPase activity from docking studies, focusing on a large area around the polyU binding site (PDB entry 1A1V; Materials and

Methods in the Supporting Information). When the new inhibitor QU663 was docked into this area, it showed striking complementarities with the enzyme region between W501 and R393: (i) establishing favorable polarized π – π interactions with W501 and F557 through the substituted quinoline ring, (ii) interacting with R393 through the negatively polarized oxygen of the hydrazide moiety and a cation– π interaction involving the pyrazine ring, (iii) establishing an ionic interaction with D496 through the protonated quinoline nitrogen, and (iv) H-bonding T298, Q434, and E493 (Figure 4E). The conformational shift of W501 with respect to the position it occupied when bound to dU₈ was noteworthy (panel D vs panel E of Figure 4). Binding of QU663 to this putative NS3h binding site would effectively allow competitive blocking of helicase function without affecting ATPase activity, according to biochemical studies (refs 4–9 of the Supporting Information). To support our hypothesis, we

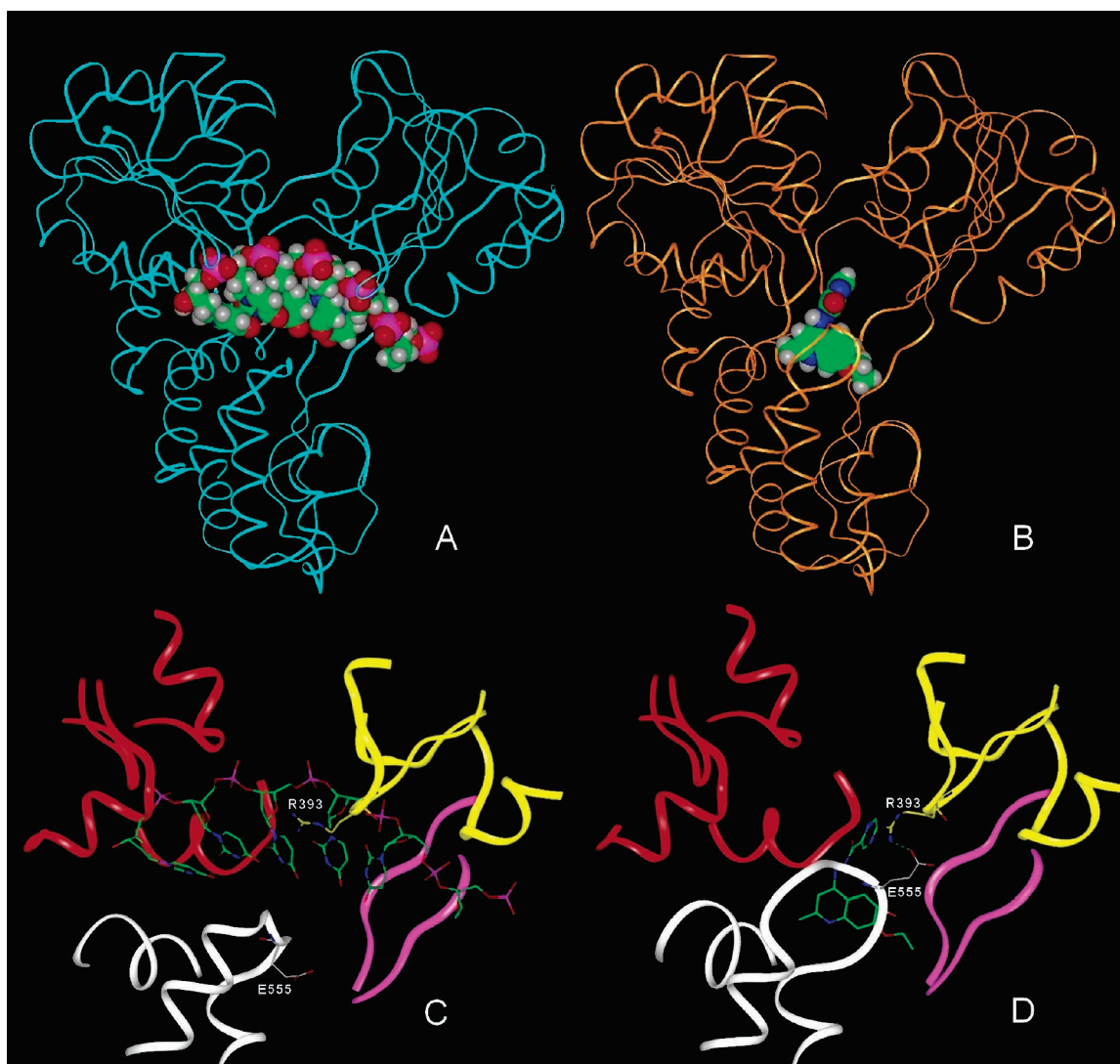


FIGURE 5: Overall view of the NS3h–dU₈ X-ray complex (A) and QU663 docked into the putative NS3h binding site (B). Ligands are colored by atom type (green for C, white for H, red for O, and blue for N). Enlarged view of the conformational shift occurring in the NS3h–QU663 docked complex (D) compared to the NS3h–dU₈ X-ray structure (C). (A and B) dU₈ and QU663 vdW volumes are displayed; the NS3h trace is cyan (A) and orange (B). (C and D) Ribbons of NS3h domains 1–3 and the Phe loop are colored red, yellow, white, and magenta, respectively. Hydrogen atoms have been omitted for clarity.

compared the X-ray structure of NS3h in complex with polyU (PDB entry 1A1V) and that of the enzyme during protease activity, when it is unable to perform its unwinding function (PDB entry 1CU1). The distance between C α atoms of R393 and E555 in 1A1V (bound to polyU) is 13.7 Å, whereas in 1CU1, domain 2 is conformationally shifted to domain 3, blocking the distance between the C α atoms of R393 and E555 at 9.5 Å (Figure 5). Docking studies showed that by interacting with the putative binding site, QU663 induced a similar conformational shift, with a distance between R393 and E555 of 8.9 Å (Figure 5), in line with its ability to competitively inhibit helicase activity, preventing NA binding. Depending on the modifications that are introduced, our results demonstrate that similar skeletons can generate anti-HIV/HCV enzyme inhibitors, paving the way for rational design of potent bifunctional antiviral drugs (for the treatment of HIV/HCV coinfections) or specific NS3h competitive inhibitors, such as QU663, the prototype of a new class of potential anti-HCV drugs.

ACKNOWLEDGMENT

We thank Dr. M. J. McGarvey (Imperial College School of Medicine, London, U.K.) for kindly providing us with expression vector pAW3 encoding the full-length HCV-NS3 protein, Dr. Alberto Bergamini and Dr. Stefano Marini (Tor Vergata University, Rome, Italy) for in vitro antiviral anti-HIV and cytotoxicity tests on QU and QX compounds, and Mrs. Helen Ampt for manuscript editing.

SUPPORTING INFORMATION AVAILABLE

Experimental details for the new compounds (molecular modeling, chemistry, HIV-1 RT enzymatic assays, anti-HIV tests, and toxicity experiments), Tables 1–4, Schemes 1 and 2, Figure 1SI, and refs 1–11. This material is available free of charge via the Internet at <http://pubs.acs.org>

REFERENCES

1. Tan, S.-L., Pause, A., Shi, Y., and Sonenberg, N. (2002) Hepatitis C therapeutics: Current status and emerging strategies, *Nat. Rev. I.*, 867–881.

2. Di Bisceglie, A. M., McHutchinson, J., and Rice, C. M. (2002) New therapeutic strategies for hepatitis C, *Hepatology* **35**, 224–231.
3. Borowski, P., Schalinski, S., and Schmitz, H. (2002) Nucleotide triphosphatase/helicase of hepatitis C virus as a target for antiviral therapy, *Antiviral Res.* **55**, 397–412.
4. Diana, G. D., and Bailey, T. R. (1997) Preparation of heterocyclic substituted carboxamides for treatment of hepatitis C, U.S. Patent 5,633,388.
5. Pollard, R. B. (1999) Analogy of human immunodeficiency virus to hepatitis C virus: The human immunodeficiency model, *Am. J. Med.* **107**, 41S–44S.
6. Maga, G., Ramunno, A., Nacci, V., Locatelli, G. A., Spadari, S., Fiorini, I., Baldanti, F., Paolucci, S., Zavattoni, M., Bergamini, A., Galletti, B., Muck, S., Hubscher, U., Giorgi, G., Guiso, G., Caccia, S., and Campiani, G. (2001) The stereoselective targeting of a specific enzyme–substrate complex is the molecular mechanism for the synergic inhibition of HIV-1 reverse transcriptase by (R)-(–)-PPO464: A novel generation of nonnucleoside inhibitors, *J. Biol. Chem.* **276**, 44653–44662.
7. Campiani, G., Aiello, F., Fabbrini, M., Morelli, E., Ramunno, A., Armaroli, S., Nacci, V., Garofalo, A., Greco, G., Novellino, E., Maga, G., Spadari, S., Bergamini, A., Ventura, L., Bongiovanni, B., Capozzi, M., Bolacchi, F., Marini, S., Coletta, M., Guiso, G., and Caccia, S. (2001) Quinoxalinyethylpyridylthioureas (QXPTs) as potent non-nucleoside HIV-1 reverse transcriptase (RT) inhibitors. Further SAR studies and identification of a novel orally bioavailable hydrazine-based antiviral agent, *J. Med. Chem.* **44**, 305–315.
8. Locatelli, G. A., Gosselin, G., Spadari, S., and Maga, G. (2001) Hepatitis C virus NS3 NTPase/helicase: Different stereoselectivity in nucleoside triphosphate utilisation suggests that NTPase and helicase activities are coupled by a nucleotide-dependent rate-limiting step, *J. Mol. Biol.* **313**, 683–694.
9. Locatelli, G. A., Spadari, S., and Maga, G. (2002) Hepatitis C virus NS3 ATPase/helicase: An ATP switch regulates the cooperativity among the different substrate binding sites, *Biochemistry* **41**, 10332–10342.
10. Maga, G., Hubscher, U., Pregnolato, M., Ubiali, D., Gosselin, G., and Spadari, S. (2001) Potentiation of inhibition of wild-type and mutant human immunodeficiency virus type 1 reverse transcriptases by combinations of nonnucleoside inhibitors and D- and L-(beta)-dideoxynucleoside triphosphate analogs, *Antimicrob. Agents Chemother.* **45**, 1192–1200.

BI047437U